

Novel PTM-TEMPO Biradical for Fast Dissolution Dynamic Nuclear Polarization.

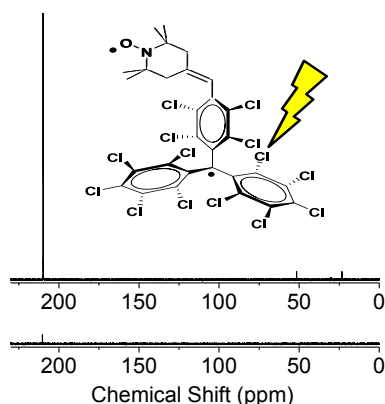
Jose-Luis Muñoz-Gómez,^{†,‡} Idefonso Marín-Montesinos,[⊥] Vega Lloveras,^{†,‡} Miquel Pons,[⊥] José Vidal-Gancedo,^{*,†,‡} and Jaume Veciana^{*,†,‡}

Institut de Ciència de Materials de Barcelona ICMA-B-CSIC; Campus UAB, 08193 Bellaterra, Barcelona (Spain) and CIBER de Bioingeniería, Biomateriales y Nanomedicina, CIBER-BBN, Barcelona (Spain) and Biomolecular NMR laboratory, Organic Chemistry Department, UB, Martí i Franquès 1-11, 08028, Barcelona, Spain.

j.vidal@icmab.es; vecianaj@icmab.es

Received Date (will be automatically inserted after manuscript is accepted)

ABSTRACT



The synthesis and characterization of a novel trityl-TEMPO biradical and the investigation of its properties as Dynamic Nuclear Polarization (DNP) polarizing agent is reported. Comparison with a structurally related monoradical (PTM=TEMPE) or mixtures of the two monoradical components reveals that the biradical has a much higher polarization efficiency and a faster polarization build-up. This offers the possibility of faster recycling further contributing to its efficiency as polarizing agent.

Dynamic nuclear polarization (DNP) has recently revealed its potential to enhance the NMR sensitivity in solids and liquids. DNP allows for the intrinsically large spin polarization of electrons to be transferred to nuclei for detection in magnetic resonance experiments with a theoretical signal enhancement of over 600 for protons and 2400 for ^{13}C . When combined with polarization at very low temperatures, sensitivity enhancements of more than 4 orders of magnitude over the Boltzmann population of the nuclear spin have been described.^{1,2,3,4,5} Steady-state enhancements of over 100 are currently achieved in solid-state experiments, equivalent to 4-5 orders of magnitude reduction in measuring times. As a result, DNP enhanced NMR has enabled studies of

previously unreachable systems, such as material surfaces⁶ or low concentration biological samples.⁷ The enhanced sensitivity offered by DNP is also being applied to metabolic imaging applications, some of which have already entered clinical trials with human subjects.⁸ The starting polarization is provided by unpaired electrons in radical species, known as polarizing agents, added to the sample of interest. The nature of the polarizing agent has a crucial role in the efficiency of DNP. For solid-state NMR biradicals formed by the combination of two nitroxides in the proper orientation and distance have proven highly efficient.^{1,9} Recent reports suggest that increasing the molecular weight of the radical improves the DNP enhancement.⁴ Monoradical trityl species are

usually chosen for the direct polarization of low γ nuclei, such as ^{13}C or ^{15}N , used for metabolic imaging applications.¹⁰ Radicals with narrow EPR lines allow efficient saturation of the majority of the unpaired electrons. However, long spin lattice relaxation times slow down the recycling of electron magnetization to enable the polarization of more nuclei. A physical mixture of two narrow-line radicals, SA-BDPA and OX63 has been shown to increase the efficiency of the polarization with respect to the individual radicals.¹¹ This effect has been assigned to the optimization of the spin lattice relaxation time (T1s) of the two radicals; the one with the longer T1s contributing to the nuclear polarization while the second one provides fast recycling. Two electron-polarization by the so called cross-effect, is a very efficient mechanism and requires that the resonant frequency of the two intervening electrons differs by exactly the nuclear frequency. This condition can usually be met in inhomogeneously broadened lines and it can be favored by the combination of distinct radicals with properly separated resonant frequencies.

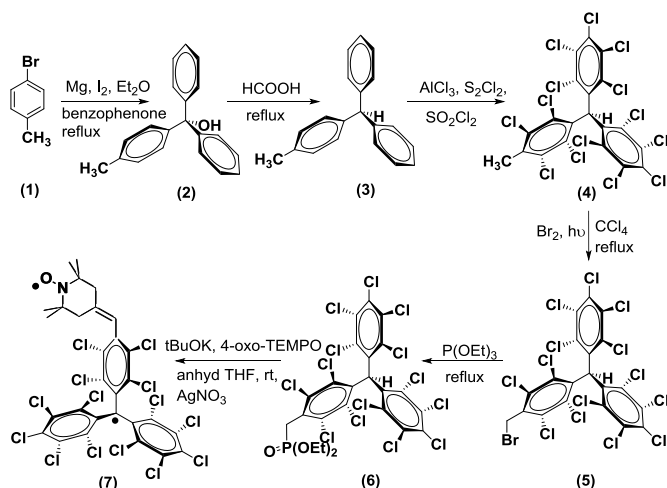
Biradicals combining a narrow-line trityl with a nitroxide, which has a much broader EPR, have been previously reported. The trityl radical used were of the Finland/OX63 family and the connection was done by direct coupling of the carboxylic acids present in the trityl radical with amino-TEMPO.⁶

Perchlorinated trityl radicals (PTM) functionalized with various carboxylic acids to improve water solubility had been shown to be efficient DNP ^{13}C polarizers. An additional polarization mechanism, named heteronuclear assisted DNP, is available in chlorinated radicals.¹²

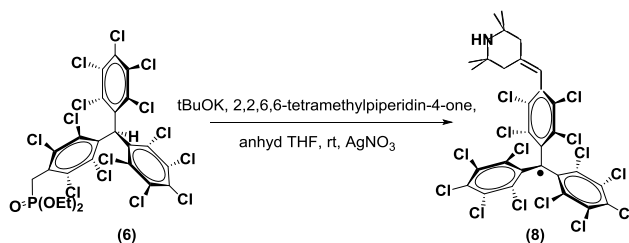
Herein we present the synthesis of novel (trans)-4-(2,2,6,6,-tetramethyl-1-piperidinyloxy)-2,3,5,6-(tetrachlorophenyl)bis (pentachloro-phenyl)methyl biradical PTM=TEMPO (**7**) and monoradical (trans)-4-(2,2,6,6,-tetramethyl-1-piperidine)-2,3,5,6-(tetrachlorophenyl)bispentachlorophenyl)methyl radical PTM=TEMPE (**8**), as well as their EPR characterization and their application as DNP polarizing agents.

The synthesis of compounds **2-6** has been previously reported in our group.¹³ The reaction between compounds **6** and 4-oxo-TEMPO (using a Wittig-Emmons-Horner reaction)¹⁴ allowed us to obtain the biradical **7** (Scheme 1) with excellent yield (82%) after the oxidation of the PTM unit. We prepared the trityl monoradical **8**, (Scheme 2), as a model compound having similar hyperfine structure than the trityl moiety of **7**, by the reaction of PTM derivative **6** with 2,2,6,6-tetramethylpiperidin-4-one using the same strategy used for the biradical **7** (see the Supporting Information). Both **7** and **8** compounds were fully characterized by EPR and MALDI-TOF spectrometries and other physicochemical techniques.

Scheme 1. Synthesis of biradical **7**.



Scheme 2. Synthesis of radical **8**.



The X-band EPR of monoradical **8** (Figure 1a) at room temperature appears as a doublet of triplets at a g -value of 2.0027 with a linewidth of 0.9 G. The origin of such lines is the coupling of the unpaired electron with the methylenic proton ($a_{\text{H}} = 6.94$ G) and with the two equivalent protons of the piperidine ring closest to the PTM subunit ($a_{\text{H}} = 1.40$ G, see the Supporting Information). The X-band EPR of biradical **7** (Figure 1b) at room temperature shows separate signals from the two radical subunits indicating that the exchange coupling between them is not significant. Thus, it exhibits three narrow lines centered at a g -value of 2.0063 with a linewidth of 0.6 G (typical of an exocyclic double bond in 4- position TEMPO radicals)^{15,16} due to the coupling with the N nucleus ($a_{\text{N}} = 14.61$ G) together with a doublet of triplets ($a_{\text{H}} = 7.89$ G and $a_{\text{H}} = 1.24$ G) at a g -value of 2.0023 due to the PTM radical subunit. The study of the EPR spectrum of biradical **7** in frozen solution (120 K) does not show resolved dipolar couplings as it fits well with the sum of the experimental TEMPO and PTM monoradicals spectra separately (see Figure S1).

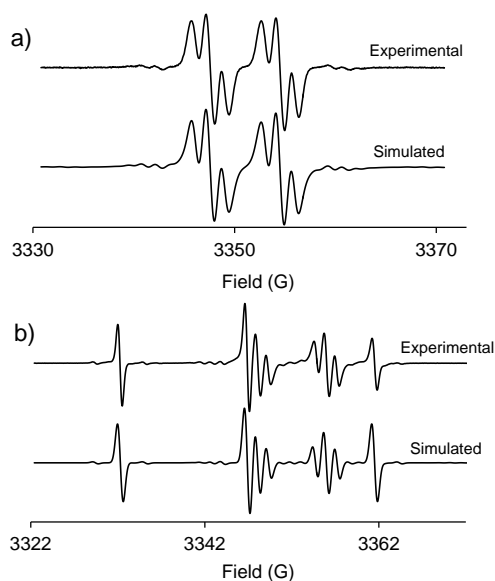


Figure 1. Experimental and simulated EPR spectra of monoradical **8** a) and biradical **7** b), in THF.

The microwave spectrum of biradical **7** (Figure S2) was acquired with a 40 mM sample. P(+) appears at 94.067 GHz while P(-) appears around 94.220 GHz. The polarization of the low frequency branch is about 4-fold higher.

In order to determine the optimum concentration of biradical **7** for the polarization of $^{13}\text{C}(2)\text{acetone}$, polarizing building curves were determined at various radical concentrations. The results are shown in Figure 2.

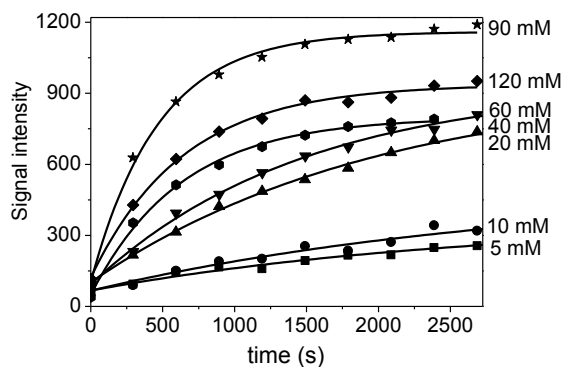


Figure 2. Polarization building-up curves (3.35 T, 1.4 K) of 100 μl of sulfolane- $^{13}\text{C}(2)\text{acetone}$ 1:1 doped with different concentrations of **7**.

The largest steady state polarization was achieved with a biradical concentration of 90 mM. The build-up time constant, extracted from the exponential fitting of the curves, decreases with radical concentration and levels off at concentrations above 60 mM (see Figure S3). The abrupt change around 60 mM suggests self-association of

7 at high concentration that, somewhat surprisingly, still sustains very efficient polarization.

The DNP efficiency of biradical **7** was compared with a model system representing the individual radical species: the monoradical TEMPO with a double bond at the 4-position and the monoradical PTM=TEMPE (**8**), each of them at the optimal concentration determined for **7**. A physical mixture of the two monoradicals at the same concentration was also studied. For each sample, the microwave DNP spectrum (see Figure S4), and polarization build-up curves (Figure 3) were measured.

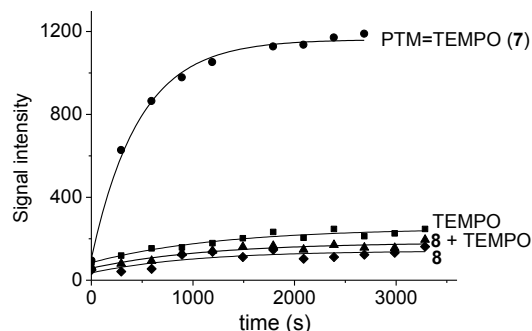


Figure 3. Polarization building curves (3.35 T, 1.4 K) of biradical **7** (90 mM) at 94.067 GHz, monoradical **8** (90 mM) at 94.08 GHz, 4-Oxo-TEMPO (90 mM) at 94.120 GHz, and a mixture of monoradical **8** and 4-Oxo-TEMPO both at 90 mM.

The polarization achieved with biradical **7** is much higher than with the individual monoradicals at the same concentration or their physical mixture, clearly showing that the high efficiency of **7** is actually due to the structure of the biradical. The fact that the optimal polarization is achieved with a high radical concentration suggests that the actual polarizing species involves supramolecular species. However, the comparison of the structurally similar species **7** and **8** suggests that the simultaneous presence of the nitroxide and PTM radicals is a key feature of the efficiency of radical **7**.

During the dissolution, transfer and spectra acquisition following low temperature polarization, the paramagnetic polarizers strongly contribute to relax the nuclear polarization. We were concerned by the possibility that the large concentration of **7** used for optimum polarization, could result in unacceptable polarization losses at this stage. In order to estimate the loss of polarization we compared the solid state polarization at low temperature with the actual signal enhancement measured in solution after the transfer process. The same comparison was carried out with 15 mM OX63 using DMSO- d_6 as a glassing agent. Figure 4a compares the build-up of $^{13}\text{C}(2)\text{acetone}$ using 90 mM **7** in 1:1 sulfolane-acetone and 15 mM OX63 in 1:1 d_6 -DMSO-acetone. Under these experimental conditions, nearly 50% more polarization was achieved with biradical **7** than with OX63. After transferring to the spectrometer by dissolving the sample in hot methanol, the intensity of the

carbonyl signal from acetone could be compared. The intensity of the carbonyl signal after a single scan is 105 times higher, in the sample polarized with **7**, after correction for the different pulse width (Figure 4 b).

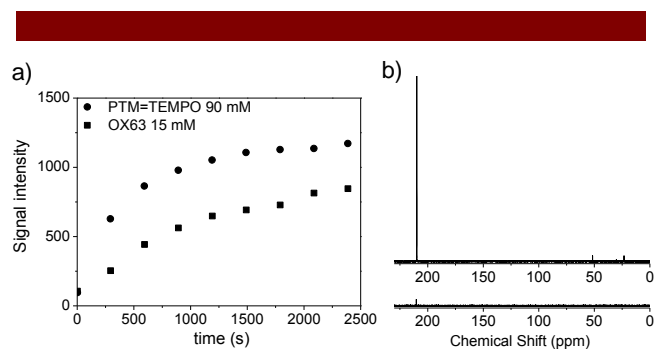


Figure 4. a) Polarization building-up curves (3.35 T, 1.4 K) of biradical **7** (circles) and OX63 (squares). b) NMR experiments. up) Hyperpolarized ^{13}C DNP-NMR spectrum ($\theta = 15^\circ$, 1 scan) of ^{13}C (2)acetone with biradical **7**, and down) Hyperpolarized ^{13}C DNP-NMR spectrum ($\theta = 35^\circ$, 1 scans) of ^{13}C (2)acetone with OX63. Optimal concentrations were used for each polarizing molecule.

After dissolution, the relative polarization increased to 105, two orders of magnitude larger. This result suggests that, in spite of the higher radical concentration in the methanol solution, **7** has a much lower capacity than OX63 to induce nuclear relaxation and the hyperpolarization of ^{13}C (2)acetone is better preserved. We suggest that the lower relaxivity of **7** in methanol could be related to the formation of radical aggregates in methanol. Indeed, EPR under the dissolution conditions clearly showed an EPR half-field transition, directly related to intermolecular interactions in the aggregates or supramolecular species.

In conclusion, a novel PTM=TEMPO biradical **7** has been prepared, characterized and tested as polarizing agent. The polarizing building curve for the optimal concentration of biradical **7** generates a better polarization than OX63 radical at its optimal concentration and it is better preserved after transferring with methanol. Thus, the presence of the TEMPO subunit has a key role, as could be seen in the polarizations provided by the monoradical **8**.

Acknowledgment. This work was supported by the grants of DGI POMAs (CTQ2010-19501) and CONSOLIDER (CTQ2006-06333), and AGAUR (2009-SGR-00516). BIO2010-15683, BioNMR 7th FP, COST TD1103 Hyperpolarization network. The DNP measurements were carried out in the NMR ICTS of the UB, part of the CCIT. The hypersense instrument was purchased with the help of Structural Funds from the EU. J. L. Muñoz thank the Networking CIBER-BBN, CSIC by the JAE Grant and I. Marín for a Juan de la Cierva contract. We thank A. Bernabé for MALDI spectrometry.

Supporting Information Available. Materials and methods, synthesis of radicals **7** and **8**, enhancement

calculation and Figures S1-S4. This material is available free of charge via the Internet at <http://pubs.acs.org>.

[†]Institut de Ciència de Materials de Barcelona ICMAB-CSIC.

[‡]CIBER-BBN.

[§]Universitat de Barcelona (UB).

(1) a) Ysacco, C.; Rizzato, E.; Virolleaud, M.-A.; Karoui, H.; Rockenbauer, A.; Moigne, F.; Siri, D.; Ouai, O.; Griffin, R. G.; Tordo P. *Phys. Chem. Chem. Phys.* **2010**, *12*, 5841-5845. b) Abragam, A.; Goldman, M. *Reports on Progress in Physics* **1976**, *41*, 395-467. c) Barnes, A. B.; Paëpe, G. D.; Wel PCAvd; Hu, K. N.; Joo, C. G.; Bajaj, V. S.; Mak-Jurkauskas, M. L.; Sirigiri, J. R.; Herzfeld, J.; Temkin, R. J.; Griffin, R. G. *Appl. Magn. Reson.* **2008**, *34*, 237-263. d) Golman, K. *Proc. Natl. Acad. Sci.* **2006**, *103*, 11270-11275. e) Golman, K.; Zandt, R. I.; Lerche, M.; Pehrson, R.; Ardenkjaer-Larsen, J. H. *Cancer Res.* **2006**, *66*, 10855-10860. f) Day, S. E.; Kettunen, M. I.; Gallagher, F. A.; Hu, D.-E.; Lerche, M.; Wolber, J.; Golman, K.; Ardenkjaer-Larsen, J. H.; Brindle, K. M. *Nat. Med.* **2007**, *13*, 1382-1387.

(2) Kiesewetter, M. K.; Corzilius, B.; Smith, A. A.; Griffin, R. G.; Swager, T. M.; *J. Am. Chem. Soc.* **2012**, *134*, 4537-4540.

(3) Han, S. T.; Griffin, R. G.; Hu, K. N.; Joo, C. G.; Joye, C. D.; Mastovsky, I.; Shapiro, M. A.; Sirigiri, J. R.; Temkin, R. J.; Torrezan, A. C.; Woskov, P. P. *Proc. Soc. Photo. Opt. Instrum. Eng.* **2006**, *6373*:63730C.

(4) a) Zagdoun, A.; Casano, G.; Ouai, O.; Schwarzwälder, M.; Rossini, A. J.; Aussenac, F.; Yulikov, M.; Jeschke, G.; Copéret, C.; Lesage, A.; et al. *J. Am. Chem. Soc.* **2013**, *135*, 12790-12797. b) Hu, K.-N.; Bajaj, V. S.; Rosay, M.; Griffin, R. G. *J. Chem. Phys.* **2007**, *126*, 044512. c) Hu, K.-N. *Solid State Nucl. Mag.* **2011**, *40*, 31-41.

(5) Lesage, A.; Lelli, M.; Gajan, D.; Caporini, M. A.; Vitzthum, V.; Miéville, P.; Alauzun, J.; Roussey, A.; Thieuleux, C.; Mehdi, A.; Bodenhausen G.; Copéret, C.; Emsley, L. *J. Am. Chem. Soc.* **2010**, *132*, 15495-15461.

(6) a) Gelis, I.; Vitzthum, V.; Dhimole, N.; Caporini, M. A.; Schedlbauer, A.; Carnevele, D.; Connell, S. R.; Fucini, P.; Bodenhausen, G. *J. Biomol. NMR* **2013**, *56*, 85-93. b) Lesage, A.; Lelli, M.; Gajan, D.; Caporini, M. A.; Vitzthum, V.; Miéville, P.; Alauzun, J.; Roussey, A.; Thieuleux, C.; Mehdi, A.; et al. *J. Am. Chem. Soc.* **2010**, *132*, 15459-15461. c) Lelli, M.; Gajan, D.; Lesage, A.; Caporini, M. A.; Vitzthum, V.; Miéville, P.; Héroguel, F.; Rascón, F.; Roussey, A.; Thieuleux, C.; et al. *J. Am. Chem. Soc.* **2011**, *133*, 2104-2107.

(7) a) Michaelis, V.K.; Smith, A.A.; Corzilius, B.; Haze, O.; Swager, T.M.; Griffin, R.G. *J. Am. Chem. Soc.* **2013**, *135*, 2935-2938. b) Lelli, M.; Gajan, D.; Lesage, A.; Caporini, M. A.; Vitzthum, V.; Miéville, P.; Héroguel, F.; Rascón, F.; Roussey, A.; Thieuleux, C.; et al. *J. Am. Chem. Soc.* **2011**, *133*, 2104-2107.

(8) a) Allouche-Arnor, H.; Wade, T.; Waldner, L. F.; Miller, V. N.; Gomori, J. M.; Katz-Brull, R. McKenzie, C. A. *Contrast Media Mol. Imaging* **2013**, *1*, 72-82. b) Nelson, S. J.; Kurhanewicz, J.; Vigneron, D. B.; Larson, P. E. Z.; Harzstark, A. L.; Ferrone, M.; van Criekinge, M.; Chang, J. W.; Bok, R.; Park, I.; et al. *Sci. Transl. Med.* **2013**, *5*, 198ra108-198ra108.

(9) a) Changsik, S.; Hu, K.-N.; Joo, C.-G.; Swager, T.M.; Griffin, R.G. *J. Am. Chem. Soc.* **2006**, *128*, 11385-11390. b) Dane, E. L.; Corzilius, B.; Rizzato, E.; Stocker, P.; Maly, T.; Smith, A. A.; Griffin, R. G.; Ouai, O.; Tordo, P.; Swager, T. M. *J. Org. Chem.* **2012**, *77*, 1789-1797.

(10) a) Gallagher, F. A.; Kettunen, M. I.; Day, S. E.; Hu, D.-E.; Ardenkjaer-Larsen, J. H.; Zandt, R. in 't; Jensen, P. R.; Karlsson, M.; Golman, K.; Lerche, M. H.; Brindle, K. M. *Nature* **2008**, *453*, 940-943. b) Ardenkjaer-Larsen, J. H.; Leach, A. M.; Clarke, N.; Urbahn, J.; Anderson, D.; Skloss, T. W. *NMR Biomed.* **2011**, *24*, 927-932.

(11) a) Gabellieri, C.; Mugnaini, V.; Paniagua, P. C.; Roques, N.; Oliveros, M.; Feliz, M.; Veciana, J.; Pons, M. *Angew. Chem. Int. Ed.* **2010**, *49*, 3360-3362. b) Paniagua, P. C.; Mugnaini, V.; Gabellieri, C.; M.; Feliz; Roques, N.; Veciana, J.; Pons, M. *Phys. Chem. Chem. Phys.* **2010**, *12*, 5824-5829.

(12) Vigier, F. M.; Shimon, D.; Mugnaini, V.; Veciana, J.; Feintuch, A.; Pons, M.; Vega, S.; Goldfarb, D. *Phys. Chem. Chem. Phys.* **2014**, *16*, 19218-19228.

(13) Rovira, C.; Ruiz-Molina, D.; Elsner, O.; Vidal-Gancedo, J.; Bonvoisin, J.; Launay, J.-P.; Veciana, J. *Chem. Eur. J.* **2001**, *7*, 240-250.

(14) Fitjer, L.; Quabeck, U. *Synthetic Commun.* **1985**, *15*, 855-864.

(15) Burks, S. R.; Makowsky, M. A.; Yaffé, Z. A.; Hoggie, C.; Tsai, P.; Muralidharan, S.; Bowman, M. K.; Kao, J. P. Y.; Rosen, G. M. *J. Org. Chem.* **2010**, *75*, 4737-4741.

(16) a) Jannin, S.; Bornet, A.; Melzi, R.; Bodenhausen, G., *Chem. Phys. Lett.* **2012**, *549*, 99-102. b) Hartmann, G.; Hubert, D.; Mango, S.; Morehouse, C. C.; Plog, K. *Nucl. Instrum. Methods* **1973**, *106*, 9-12.